JOURNAL OF APPLIED ELECTROCHEMISTRY 24 (1994) 350–354

Effect of some variables on the electroplating of zinc from acidic acetate baths

S. S. ABD EL REHIM, S. M. ABD EL WAHAAB, E. E. FOUAD, H. H. HASSAN

Department of Chemistry, Faculty of Science, Ain Shams University, Cairo, Egypt

Received 5 April 1993; revised 17 August 1993

Electroplating of zinc onto steel substrates from baths containing zinc acetate and acetic acid has been investigated under different conditions of bath composition, current density, temperature and superimposed sinusoidal a.c. on d.c. A detailed study has been made of the influence of these variables on the potentiodynamic cathodic polarization, cathodic current efficiency and the throwing power of these baths. The surface morphology of the deposits was examined by scanning electron microscopy and crystal structure by X-ray.

1. Introduction

The high corrosion resistance and wide range of applications of zinc and its alloys make their electroplating of practical importance. Zinc can be electroplated from alkaline and acid baths [1, 2]. Cyanide baths are the most common alkaline baths. These baths have good throwing power and are usually used to electroplate irregularly shaped articles. However, their high toxicity is a serious disadvantage.

Among the acid baths used are sulphate baths [3–5] and chloride baths [6, 7]. These usually operate at high current densities at good efficiency with low operating costs [1]. Deposits are coarse grained, unless organic additives are used. Acid baths have poor throwing power.

Continuing our work on the electroplating of some metals and alloys from acetate baths [8–10], the present work was undertaken to study the electroplating of zinc from baths containing zinc acetate and acetic acid under various plating conditions.

2. Experimental details

Experiments were conducted in solutions containing $Zn(CH_3COO)_2 \cdot 2H_2O$ (10–120 g dm^{-3}) and glacial CH_3COOH (10–80 cm^3 dm^{-3}). All solutions were freshly made from A.R. chemicals and doubly distilled water. The experimental set-up for the electrodeposition consisted of a Perspex rectangular cell provided with a plane parallel steel sheet cathode and a platinum sheet anode. Each electrode had dimensions of 2.5 cm × 3 cm and filled the cross section of the cell. Before each run, the electrodes were mechanically polished with 600 mesh emery paper, washed with distilled water, rinsed with ethanol and the weight of the cathode was determined. Direct current (d.c.) was supplied by a 12 V battery. The plating duration was 12 min. Experiments were carried out at the required temperature ±0.5° C with the help of an air thermostat. In some experiments a sinusoidal alternating current of constant frequency (60 Hz) was superimposed on the d.c. The a.c. was supplied by an a.c. generator type GF20 Rc and connected directly to the cathode and the anode. To achieve separation of a.c. and d.c. circuits, a capacitor (100 μF) was introduced into the a.c. circuit and an inductor (10.5 H) into the d.c. circuit.

Potentiodynamic cathodic polarization measurements were performed into the rectangular cell. A potentiostat (Wenking Model POS 73) was used as the d.c. source. Potentials were measured against a saturated calomel reference electrode. To avoid contamination, the reference electrode was connected to the working steel cathode via a bridge provided with Luggin–Haber tip and filled with the solution under test. The potential-current density curves were recorded using an X–Y recorder (Series 2000, Ominographic).

The throwing power (T.P.) of the bath was measured in a rectangular cell (Haring Blum cell) in which the platinum sheet anode was placed between two parallel steel cathodes. One of the cathodes was nearer to the anode than the other. The distance ratio, L, was 1 : 1–1 : 4. The throwing power was calculated using Field's formula [11]: T.P. $= (L - M)/(L + M - 2) \times 100$, where M is the metal distribution ratio, ω_n/ω_f, where ω_n and ω_f are the weights of zinc deposited on the near and far cathode, respectively.

X-ray analysis of the as-plated zinc was carried out using a Philips diffractometer (40 kV, 25 mA) with nickel filter and copper radiation. The morphology of the deposits was examined using a scanning electron microscope (JEOL SEM T200).

3. Results and discussion

3.1. *Potentiodynamic polarization curves*

The potentiodynamic polarization curves for zinc electrodeposition were recorded under different

0021-891X 1994 Chapman & Hall

conditions. The curves were swept from zero current potential (rest potential) up to −1350 mV vs SCE at a scan rate of $1\,mV\,s^{-1}$. Some of these curves are given in Figs 1–3. The polarization curves are characterized by the occurrence of two cathodic peaks C_I and C_I, prior to the sudden rise of the cathodic current density at the deposition potential of zinc metal. Within the potential range of the first cathodic peak, C_I, hydrogen evolution was observed. Therefore, the first peak, C_I, is assigned to the discharge of H^+. However, assuming that the discharge of $Zn^{2+} \rightarrow Zn$ is improbable owing to the high energy barrier to be surmounted [12], it is generally accepted that the electroreduction of bivalent zinc ions takes place in two stages [13, 14].

$$Zn^{2+} + e^- \longrightarrow Zn^+_{ads}$$

$$Zn^+_{ads} + e^- \longrightarrow Zn$$

In the second stage, the adsorbed Zn^+_{ads} diffuses to sites of growth and electrocrystallizes at the deposition potential. The appearance of the second cathodic peak, C_{II}, can be related to the formation of the intermediate Zn^+_{ads}.

Figure 1 shows the effect of bath concentration on the characteristic features of the cathodic polarization curves. Increasing the Zn^{2+} content in the bath decreases the height of the peak C_I but increases the height of the peak C_{II} and shifts the deposition potential towards the less negative value. These results can be attributed to an increase in relative concentration of Zn^{2+} in the diffusion layer and this is reflected in a decrease in concentration polarization associated with zinc deposition. Nevertheless, the reverse was observed with increasing acid concentration in the bath.

Figure 2 illustrates the effect of temperature on the cathodic polarization behaviour. It is clear that the peak current of the two peaks C_I and C_{II} increase and their corresponding peak potentials, as well as

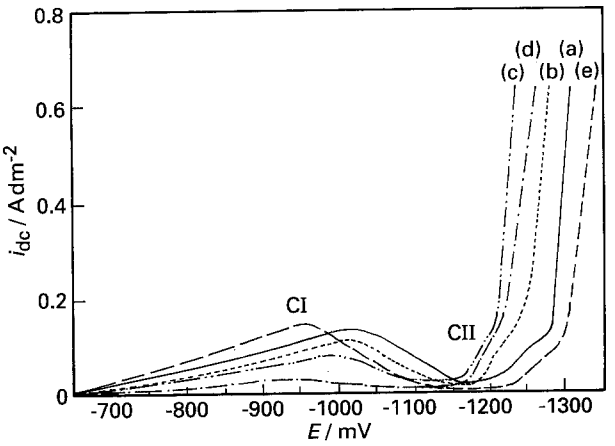

Fig. 1. Potentiodynamic cathodic polarization curves for the electrodeposition of zinc at 25° C, $\nu = 1\,mV\,s^{-1}$. Curve (a) $10\,g\,dm^{-3}$ $Zn(CH_3COO)_2 2H_2O$ and $10\,cm^3\,dm^{-3}$ CH_3COOH; curve (b) $50\,g\,dm^{-3}$ $Zn(CH_3COO)_2 2H_2O$ and $10\,cm^3\,dm^{-3}$ CH_3COOH; curve (c) $100\,g\,dm^{-3}$ $Zn(CH_3COO)_2\ 2H_2O$ and $10\,cm^3\,dm^{-3}$ CH_3COOH; curve (d) $50\,g\,dm^{-3}$ $Zn(CH_3COO)_2 2H_2O$ and $5\,cm^3\,dm^{-3}$ CH_3COOH; curve (e) $50\,g\,dm^{-3}$ $Zn(CH_3COOH)_2 \cdot 2H_2O$ and $80\,cm^3\,dm^{-3}$.

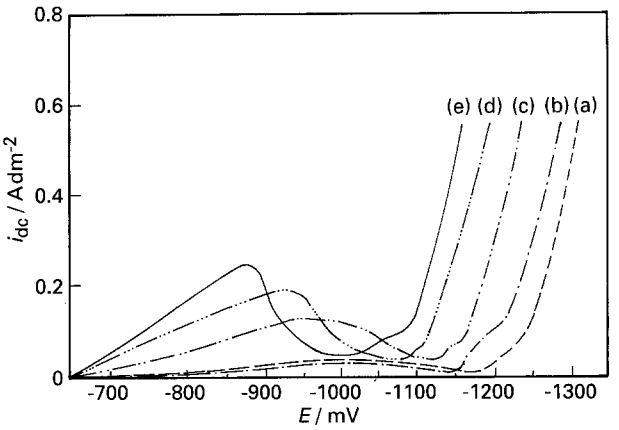

Fig. 2. Effect of temperature on potentiodynamic cathodic polarization curves for the electrodeposition of zinc from solution containing $50\,g\,dm^{-3}$ $Zn(CH_3COO)_2 2H_2O$, $10\,cm^3\,dm^{-3}$ CH_3COOH, $\nu = 1\,mV\,s^{-1}$. Curves: (a) 17° C; (b) 25° C; (c) 35° C; (d) 47° C; (e) 55° C.

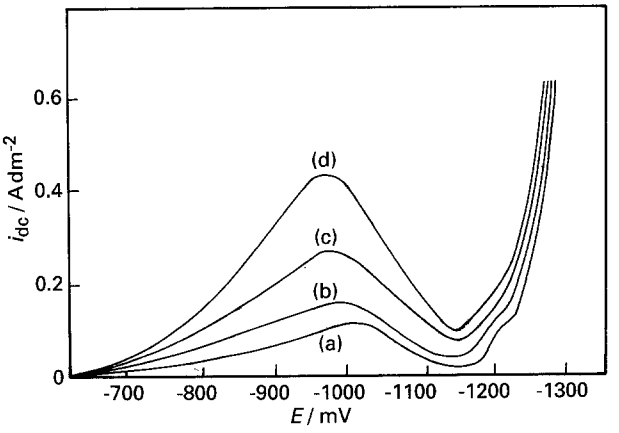

Fig. 3. Effect of superimposed a.c. (60 Hz) on potentiodynamic cathodic polarization curves for the electrodeposition of zinc from solution containing $50\,g\,dm^{-3}$ $Zn(CH_3COO)_2 2H_2O$ and $10\,cm^3\,dm^{-3}$ CH_3COOH at 25° C, $\nu = 1\,mV\,s^{-1}$. Current density, i: (a) 0, (b) 2.0, (c) 4.8 and (d) $6.9\,A\,dm^{-2}$.

the deposition potential, shift to less negative values with increasing temperature. The effect of temperature is more pronounced on the height of peak C_I than that of peak C_{II}. An increase in temperature enhances the concentration of the two ions in the diffusion layer as a result of increasing the diffusion rates. An increase in temperature also causes a decrease in the activation polarization at the cathode interface.

Figure 3 shows the cathodic polarization curves under a.c. Superimposing a.c. on d.c. increases the heights of the two current peaks and depolarizes the reduction potentials. The magnitude of these changes increases with increasing a.c. density. Such effects of a.c. can be explained in terms of the nonlinear character of the cathode [15, 16]. Accordingly, the sine wave of the a.c. suffers distortion at the electrode surface. In turn the potential fluctuates periodically, giving rise to an average potential which, in the present system, is less negative than for d.c. alone.

3.2. *Cathodic current efficiency*

The cathodic current efficiency, F, for zinc deposition from these baths was determined under the effect of

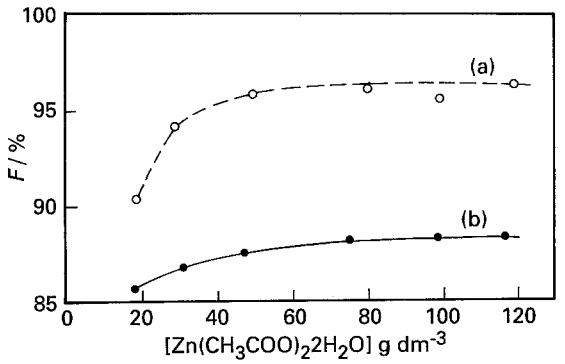

Fig. 4. Effect of $Zn(CH_3COO)_2 2H_2O$ concentration on the cathodic current efficiency of zinc deposition at 25° C, $i_{d.c.} = 2.7\,A\,dm^{-2}$. Curves: (a) 10, (b) $60\,cm^3\,dm^{-3}$ CH_3COOH.

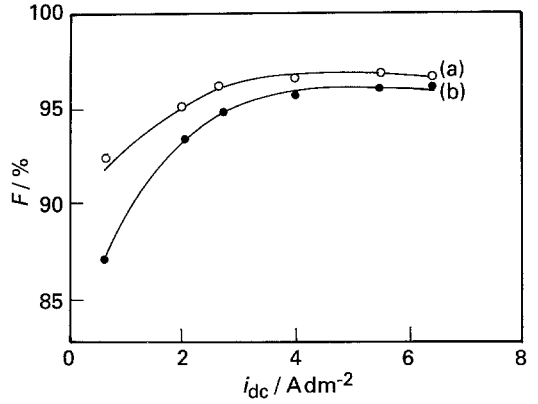

Fig. 5. Effect of $i_{d.c.}$ density on the cathodic current efficiency for zinc deposition at 25° C. Curves: (a) $50\,g\,dm^{-3}$ $Zn(CH_3COO)_2 2H_2O$ and $10\,cm^3\,dm^{-3}$ CH_3COOH; (b) $70\,g\,dm^{-3}$ $Zn(CH_3COO)_2 2H_2O$ and $10\,cm^3\,dm^{-3}$ CH_3COOH.

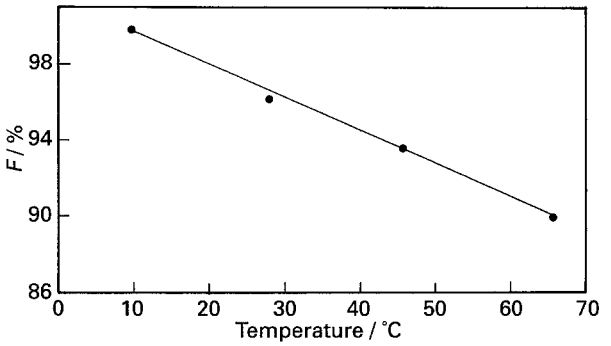

Fig. 6. Effect of temperature on the cathodic current efficiency for zinc deposition from solution containing $50\,g\,dm^{-3}$ $Zn(CH_3COO)_2 2H_2O$ and $10\,cm^3\,dm^{-3}$ CH_3COOH, $i_{d.c.} = 2.7\,A\,dm^{-2}$.

different variables. In general, the values of F are high, but less than 100%, denoting simultaneous discharge of hydrogen, as expected from the cathodic polarization curves. Figure 4 shows that the efficiency, F, increases with increasing the concentration of Zn^{2+} up to about $50\,g\,dm^{-3}$ and then levels off. The improvement in the efficiency may be due to decreased zinc cathodic polarization in addition to the increase in hydrogen overpotential. The reverse result was obtained by increasing the acid content in the bath. Figure 5 illustrates the influence of increasing the deposition current density on the values of F.

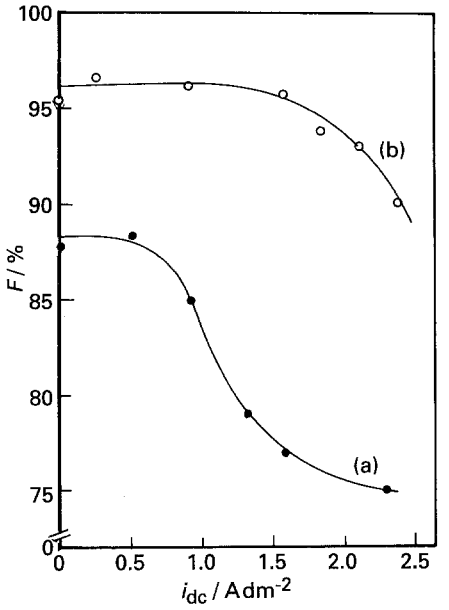

Fig. 7. Effect of $i_{a.c.}$ density (60 Hz) on the cathodic current efficiency for zinc deposition from solution containing $50\,g\,dm^{-3}$ $Zn(CH_3COO)_2 2H_2O$ and $10\,cm^3\,dm^{-3}$ CH_3COOH, 25° C. Current density, $i_{d.c.}$ (a) 0.7 and (b) $2.0\,A\,dm^{-2}$.

Initially, the efficiency increased with increasing current density and then levelled off up to a certain critical value, beyond which dendrite formation occurred. The higher the Zn^{2+} concentration, the higher the critical current density and hence the delay in dendrite formation. Figure 6 shows the relation between deposition efficiency and temperature of the bath. Increasing temperature has a greater depolarizing effect on hydrogen evolution than on zinc deposition and a decrease in the efficiency of zinc deposition with temperature might be expected. Figure 7 shows the influence of superimposed a.c. on the values of F for zinc deposition. The efficiency decreases with increasing a.c. density. This effect of a.c. can be related to its effect on cathodic polarization and also to the possibility of zinc dissolution during the anodic half cycle.

3.3. *Structure and morphology of the deposits*

The zinc deposits obtained from these electrolytes were generally adherent, smooth and grey in appearance. Increasing the Zn^{2+} concentration and superimposing a.c. on d.c. enhanced the smoothness and brightness. At temperatures higher than 40° C, the deposits turned black.

X-ray diffraction measurements were conducted on some plates deposited from selected solutions and under different operating conditions. For example, the results obtained for the sample deposited from solution containing $50\,g\,dm^{-3}$ Zn $(CH_3COO)_2 \cdot 2H_2O$ and $10\,cm^3\,dm^{-3}$ CH_3COOH at $i_{d.c.} = 2.667\,A\,dm^{-2}$, 25° C and a duration of 10 min are given in Table 1. From the diffractograms obtained it appears that, irrespective of the conditions, all the deposits are crystalline and are also plated in the hexagonal structure.

Table 1. X-ray diffraction data for electrodeposited zinc from a solution containing 50 g dm^{-3} $Zn(CH_3COO)_2 \cdot 2H_2O$ and 10 cm^2 dm^{-3} CH_3COOH at $i_{d.c.}$ = 2.667 A dm^{-2}, 25° C and 10 min duration

d-spacing/nm	*Relative intensity* I/I_0	*h k l*	*Lattice parameters/nm*		*Structure*
			a	*c*	
0.2478	53	0 0 2	0.330	0.52	hexagonal
0.2091	100	1 0 1			
0.1332	21	1 1 0			
0.1173	23	1 1 2			

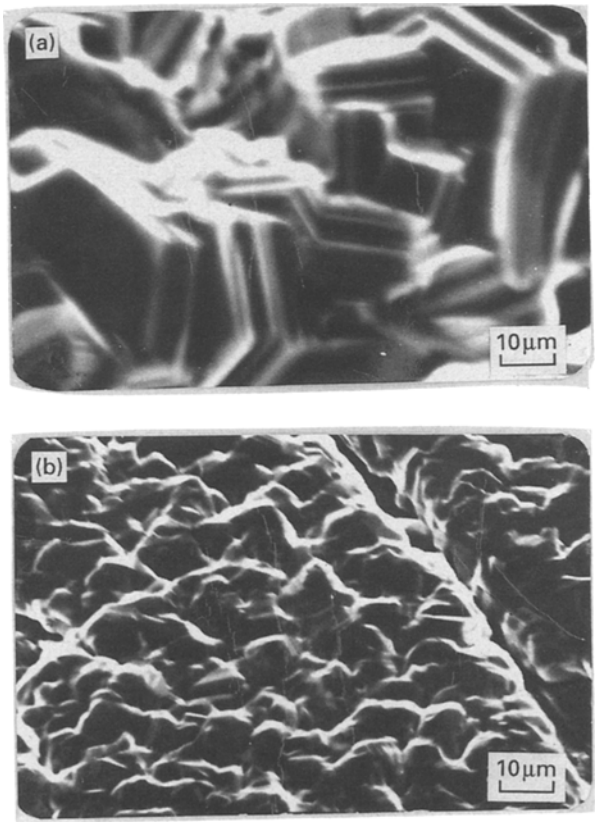

Fig. 8. Scanning electron photomicrograph of the as-deposited zinc from solution containing 50 g dm^{-3} $Zn(CH_3COO)_2 2H_2O$ and 10 cm^3 dm^{-3} CH_3COOH at 20° C. Current density, $i_{d.c.}$ (a) 2.667 and (b) 2.667 A dm^{-2} superimposed with $i_{a.c.}$ = 2.4 A dm^{-2} (H_3 = 60).

Figure 8 shows some SEM micrographs of the as-plated zinc obtained under different conditions. In general, the deposits contain randomly distributed hexagonal crystals with definite boundaries. The crystals are oriented at different angles to the basis surface. Increasing the Zn^{2+} concentration gives uniform and fine grained deposits; the same effects are produced by increasing the current density. On the other hand, increasing the acid content or raising the temperature promotes the formation of coarse grained deposits.

Superimposing a.c. on d.c. gives very fine grains and level deposits, though some surface cracks are also observed. The deposition of fine grains may be due to an enhancement in the rate of nucleation during the cathodic deposition reaction under the influence of superimposed a.c. [17].

3.4. *Throwing power of the plating bath*

The throwing power (T.P.) of the acidic acetate bath was measured using Haring Blum cell. Table 2 includes the numerical values of the T.P. of this bath computed by using the empirical Field formula at the distance ratio 1:3 under the influence of some plating variables. Figure 9 shows some linear plots between the metal distribution ratio, M, and the linear ratio, L (1:1–1:4). The reciprocals of the slopes (i.e. linear throwing index T.I.) were used as indicators of throwing power [18]. The values of T.I. are also listed in Table 2. The data reveal that this bath has low throwing power, as do other acidic zinc plating baths. In some cases, negative values of T.P. were obtained. This means that here the weight of the deposit at the far cathode is even less than

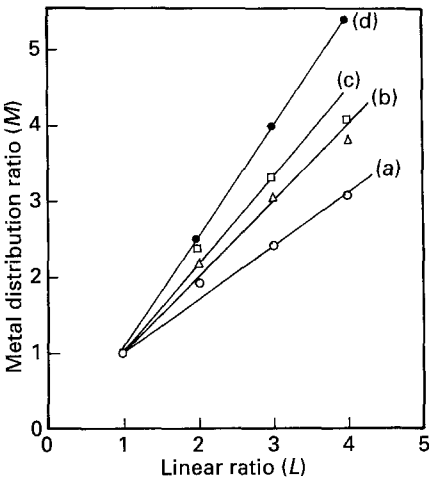

Fig. 9. Metal distribution ratio M against linear ratio L. Curves: (a) 10 g dm^{-3} $Zn(CH_3COO)_2 2H_2O$ and 10 cm^3 dm^{-3} CH_3COOH at 25° C; (b) 50 g dm^{-3} $Zn(CH_3COO)_2 2H_2O$ and 10 cm^3 dm^{-3} CH_3COOH at 25° C; (c) 80 g dm^{-3} $Zn(CH_3COO)_2 2H_2O$ and 10 cm^3 dm^{-3} CH_3COOH at 25° C; (d) 50 g dm^{-3} $Zn(CH_3COO)_2 2H_2O$ and 10 cm^3 dm^{-3} CH_3COOH at 63° C.

Table 2. Effect of some plating variables on the throwing power T.P.% and throwing index T.I. for zinc electrodeposition

Solution	$i_{d.c.}$/A dm^{-2}	*Temp./°C*	*Time/min*	*T.P./%*	*T.I.*
10 g dm^{-3} Zn $(CH_3COO)_2 2H_2O$ and 10 cm^3 dm^{-3} CH_3COOH	2.667	28	10	16.27	1.25
50 g dm^{-3} Zn $(CH_3COO)_2 2H_2O$ and 10 cm^3 dm^{-3} CH_3COOH	2.667	28	10	−0.99	0.99
50 g dm^{-3} Zn $(CH_3COO)_2 2H_2O$ and 30 cm^3 dm^{-3} CH_3COOH	2.667	28	10	3.89	1.05
50 g dm^{-3} Zn $(CH_3COO)_2 2H_2O$ and 10 cm^3 dm^{-3} CH_3COOH	2.667	63	10	−2.16	0.67
50 g dm^{-3} Zn $(CH_3COO)_2 2H_2O$ and 10 cm^3 dm^{-3} CH_3COOH	0.667	28	10	8.69	0.99

predicted for primary current distribution. Increasing the Zn^{2+} concentration and decreasing the acid concentration caused a decrease in the values of both T.P. and T.I. as a result of decreasing the cathodic polarization. Increasing the current density of deposition improves the throwing power of the bath as a result of increasing the cathodic polarization. Raising the bath temperature lowers the throwing power of the bath due to decreasing polarization, even though increasing the temperature enhances the conductivity of the solution.

4. Conclusion

Adherent and smooth deposits of zinc were successfully electroplated onto steel substrates from the acidic acetate bath studied. The bath is characterized by high cathodic current efficiency but low throwing power. The deposits were sound and satisfactory under most conditions. An explanation has been offered for the various trends observed during the investigation in the light of cathodic polarization phenomena. The optimum plating variables are: $Zn(CH_3COO)_2 \cdot 2H_2O$, 50 g dm^{-3}; CH_3COOH 10 cm^3 dm^{-3}; c.d. 2.66 A dm^{-2}; t 10 min; temperature 25° C.

References

[1] R. M. Burns and W. W. Bradley, 'Protective Coatings for Metals' Reinhold, New York (1967).
[2] F. A. Lowenheim, 'Modern Electroplating', 2nd edn, John Wiley & Sons, New York (1963).
[3] I. W. Wark, *J. Appl. Electrochem.* **9** (1979) 721.
[4] G. C. Ye, Y. U. Kim and D. C. Ahn, *Kumsok Pyomyon Choli* **18** (1985) 53.
[5] N. M. Dubina, S. V. Plyasorskaya, Z. A. Kadymova and S. A. Chudngi, *USSR Technol. Organ. Proizvad.* **3** (1987) 49.
[6] H. Farid and N. Hiroomi, *Met. Finish.* **86** (1988) 33.
[7] E. A. Blount, *Electroplat. Met. Finish.* **23** (1970) 42.
[8] S. M. Abd El Wahaab, A. M. Abd El Halim, S. S. Abd El Rehim and E. A. Abd El Meguid, *Surf. Technol.* **29** (1986) 313.
[9] *Idem, J. Appl. Electrochem.* **17** (1987) 49.
[10] *Idem, ibid.* **17** (1987) 667.
[11] S. Field, *Met. Ind., London* **44** (1934) 416.
[12] L. P. Shul'gin and V. I. Petrova, *Russian J. Phys. Chem.* **47** (1973) 1148.
[13] T. Hurien and E. Eriksrud, *J. Electroanal. Chem.* **45** (1973) 405.
[14] K. E. Heusler and R. Kondler, *Electrochim. Acta*, **18** (1973) 855.
[15] J. Devay and S. S. Abd El Rehim, *Maguar Kem. Foly.* **75** (1969) 131.
[16] S. S. Abd El Rehim and A. M. Abd El Halim, *Acta Chim. Hung.* **80** (1974) 65.
[17] D. T. Chin and S. Venkatesh, *J. Electrochem. Soc.* **128** (1981) 1439.
[18] R. V. Jelinek and H. F. David, *ibid.* **104** (1957) 279.